N-Terminal Domain of Phosphodiesterase-11A4 (PDE11A4) Decreases Affinity of the Catalytic Site for Substrates and Tadalafil, and is Involved in Oligomerization†

James L. Weeks, II, Roya Zoraghi,‡ Sharron H. Francis, and Jackie D. Corbin*

Deptartment of Molecular Physiology and Biophysics, Vanderbilt University School of Medicine, 702 Light Hall, Nashville, Tennessee 37232-0615

Received May 19, 2007; Revised Manuscript Received June 27, 2007

ABSTRACT: The phosphodiesterase-11A (PDE11) family consists of four splice variants (PDE11A1−PDE11A4) that contain a conserved carboxyl-terminal (C-terminal) catalytic domain that hydrolyzes cAMP and cGMP; the amino-termini (N-termini) vary in length and amino acid sequence. PDE11A2, PDE11A3, and PDE11A4 contain one or more GAF (cGMP-binding phosphodiesterase, *Anabaena* adenylyl cyclase, and *Escherichia coli* FhlA) subdomains. In the present study, PDE11A1 and PDE11A2 demonstrated higher affinity for cAMP and cGMP when directly compared to that of the longest isoform, PDE11A4. Moreover, PDE11A3, PDE11A2, and PDE11A1, which contain progressively shorter N-termini, were more sensitive than PDE11A4 to inhibition by two structurally unrelated inhibitors, tadalafil (Cialis) and vardenafil (Levitra). The substrate and inhibitor affinity differences among the PDE11 isozymes could not be ascribed to differences in their quaternary structure since PDE11A4, PDE11A3, and PDE11A2 were determined to be dimers, and PDE11A1 was a tetramer. These data also demonstrate that PDE11 isozymes containing at least 123 C-terminal amino acids of the GAF-B domain are stable oligomers and that GAF-A is not required for oligomerization. The isolated PDE11 catalytic domain (Met-563-Asn-934) displayed both monomeric and dimeric forms, and upon dilution, this domain was primarily monomeric, indicating that the main oligomerization contacts are within the N-termini of PDE isozymes. This report is the first to describe an inhibitory effect of the N-terminal region of PDE11A4 on the affinity of the catalytic domain for both substrates and inhibitors and the first to define the quaternary structure and the regions that contribute to this structure within the human PDE11A family.

Cyclic AMP (cAMP[1]) and cyclic GMP (cGMP) are cyclic nucleotide (CN) second messengers that modulate virtually all physiological processes. Intracellular levels of CNs are dependent primarily on two opposing enzyme activities: CN synthesis by adenylyl or guanylyl cyclases and CN hydrolysis by CN phosphodiesterases (CN-PDEs). CN-PDEs consist of a superfamily of metallophosphohydrolases that catalyze hydrolysis of the cyclic phosphate bond of cAMP, cGMP, or both CNs to their respective 5′ noncyclic forms (*1*−*6*). Given the pivotal role that PDEs play in modulating cellular CN levels and their potential as pharmacological targets, it is important to determine the biochemical characteristics that provide for their regulatory and catalytic mechanisms (*7*). Four human PDE11 isozymes (Figure 1) have been described (PDE11A1−PDE11A4), which arise from a single gene via alternative mRNA splicing. These isozymes are considered to have dual specificity since they hydrolyze both cAMP and cGMP. All four human PDE11 isozymes consist of a conserved C-terminal PDE catalytic domain that hydrolyzes cAMP and cGMP, and N-terminal domains of varying lengths. In addition, each of the PDE11 isozymes contains either intact GAFs or portions of a GAF (cGMP-binding phosphodiesterase, *Anabaena* adenylyl cyclase, and *Escherichia coli* FhlA) sequence (Figure 1) (*8*−*12*). GAFs subserve variable functions in proteins, but most GAFs in mammalian proteins are found in CN-PDEs (*1*, *13*). Human PDE11A4 consists of 934 amino acids with an N-terminal domain of unknown functions and a C-terminal catalytic domain that hydrolyzes CN substrates; the sequence includes two consensus phosphorylation sites for cAMP-dependent protein kinase (PKA) or cGMP-dependent protein kinase (PKG). On the basis of the SMART domain prediction program, PDE11A4 contains two GAF subdomains (termed GAF-A and GAF-B) that extend from residues 217 to 380 and 402 to 568, respectively. In PDE11A3, there is a partial GAF-A subdomain that shares the final 75 residues of GAF-A of PDE11A4; the 54 residues of PDE11A3 N-terminal to these conserved 75 residues are unique and absent in the other PDE11 isozymes (*9*, *10*). PDE11A1 and PDE11A2 are

† This work was supported by American Heart Association Predoctoral Fellowship 0515286B and an NIH training grant in Vascular Biology 5T32HL07752. This work was also supported by NIH grants DK40299 and DK58277.

* To whom correspondence should be addressed. Phone: 615-322-4382. Fax: 615-322-7236. E-mail: Jackie.Corbin@vanderbilt.edu.

‡ Present address: University of British Columbia, PREPARE Lab, VGH Research Pavilion, Room 687−828, West 10th Avenue, Vancouver, B.C. V5Z 1L8.

[1] Abbreviations: PDE, cyclic nucleotide phosphodiesterase; GAF, mammalian cGMP-binding phosphodiesterase, *Anabaena* adenylyl cyclase, and *Escherichia coli* FhlA; PKA, cAMP-dependent protein kinase; PKG, cGMP-dependent protein kinase; Sf9, *Spodoptera frugiperda*; PAGE, polyacrylamide gel electrophoresis; cGMP, cyclic GMP; cAMP, cyclic AMP; CN, cyclic nucleotide; Ni-NTA, nickel-nitriloacetic acid; Tris-HCl, Tris (hydroxymethyl)aminomethane hydrochloride; E64, L-*trans*-epoxysuccinyl-leucylamide-(4-guanido)-butane; AEBSF, 4-(2-aminoethyl) benzenesulfonyl fluoride HCl; PMSF, phenylmethylsulphonyl fluoride.

10.1021/bi7009629 CCC: $37.00
Published on Web 08/16/2007

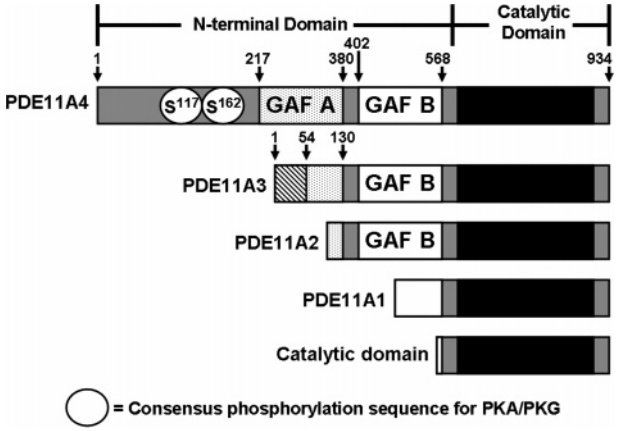

FIGURE 1: Schematic representation of human PDE11A isozymes and the isolated PDE11 catalytic domain. PDE11A1-PDE11A4 were expressed in Sf9 cells via a baculovirus expression system as outlined under Experimental Procedures. The isolated PDE11 catalytic domain was expressed in *E. coli* as described in Experimental Procedures. Residue numbers of PDE11A4 and PDE11A3 are shown above the depictions. Residues contained in PDE11A2, PDE11A1, and the catalytic domain are all present in PDE11A4, while PDE11A3 contains a unique 54 residue insert (crosshatch pattern) at the N-terminus. The black shaded region represents the conserved PDE11 catalytic domain.

N-terminal truncated forms of PDE11A4; the PDE11A2 N-terminal sequence begins with the C-terminal 22 residues of GAF-A found in PDE11A4, and the remainder of the sequence is identical to that of PDE11A4. PDE11A1 has no GAF-A sequence, and the N-terminus begins with the last 123 residues of GAF-B found in the other isozymes (*8*, *10*−*12*).

One or more of the GAF subdomains in the N-terminal domains of PDE2, PDE5, and PDE6 are involved in high-affinity allosteric cGMP binding and/or dimerization of these enzymes (*14*−*18*). Subdomains in the N-terminal region of the PDE4 family also contribute to oligomerization. A study with a chimeric protein comprising residues 1−568 of the N-terminal domain of PDE11A4 fused with the catalytic domain of the cyaB1 adenylyl cyclase of *Anabaena* has demonstrated that cGMP specifically stimulates the activity of the cyclase and implies that cGMP can bind to the N-terminus of PDE11A4, albeit with low affinity (*19*). On the basis of the GAF-B sequence of PDE2A and the GAF-A sequence of PDE5A, both of which bind cGMP with high affinity, a consensus cGMP-binding motif of 11 residues has been proposed (*16*). The GAF-A domain of PDE11A4 has different amino acids in 2 of the 11 positions of this motif, while the GAF-B has different amino acids in 6 of these positions. Whether either GAF subdomain interacts with CN in an intact PDE11A isozyme has not been demonstrated.

Oligomerization of the PDE4 family is also mediated by subdomains in its N-terminal region. The majority of PDEs studied to date behave as oligomers in solution, leading to the suggestion that oligomerization plays an important, yet undiscovered, function (*20*). Recently, the oligomeric state of the PDE4 and PDE5 family has been shown to influence regulatory properties and potency of inhibitors, and the oligomeric states of other enzymes, for example, PKG, are an important determinant of enzymatic function (*20*−*23*). Of the four human PDE11A isozymes, several recent reports suggest that the longest isozyme, PDE11A4, is most readily detected in human tissues (*24*, *25*). The PDE5 catalytic site and the PDE11 catalytic site have the highest sequence identity (51%) within the mammalian PDE superfamily, and moderate cross-reactivity of the PDE5-selective inhibitor Cialis (tadalafil, Lilly-ICOS) has been demonstrated (*5*), although the extent of cross-reactivity has not been quantified among all PDE11 isozymes. To provide insight into the influence of the N-terminal domains of PDE11 isozymes on catalytic function, inhibitor potency, and the potential relationship between the oligomeric state and these properties, we have characterized in a head-to-head manner all natural human PDE11A isozymes as well as the isolated PDE11 catalytic domain.

EXPERIMENTAL PROCEDURES

Materials. Cyclic AMP, cGMP, apoferritin, cytochrome *c*, phosphorylase *b*, bovine serum albumin, soybean trypsin inhibitor, catalase, ovalbumin, penicillin, streptomycin, amphotericin B, Triton X-100, and protease inhibitors (E-64, AEBSF or PMSF, leupeptin, and pepstatin-A) were purchased from Sigma (St. Louis, MO). Complete EDTA-free protease inhibitor cocktail was from Roche Diagnostics (Indianapolis, IN) and was used at the manufacturers suggested concentration. Crystalline bovine hemoglobin was from Nutritional Biochemicals Corp. (Cleaveland, OH). All restriction endonucleases were from New England Biolabs (Ipswich, MA). Tritiated cAMP and cGMP, DEAE-Sephacel, all gel filtration resins, and secondary antibodies were from Amersham Biosciences (Piscataway, NJ). Western Lightning Chemiluminescence kit was from Perkin-Elmer Life Sciences (Boston, MA). Isopropyl-β-D-thiogalactopyranoside (IPTG) was from RPI Biochemicals (Natick, MA). Tadalafil (Cialis, Lilly-ICOS Co.) was synthesized on the basis of the procedure by Daugan et. al (*26*). Vardenafil was a generous gift from Bayer AG (Wuppertal, Germany). Nickel-NTA affinity resin was from Qiagen (Valencia, CA). BL21 (DE3) Codonplus RIL cells were from Stratagene (La Jolla, CA). Baculovirus expression vector systems were from Invitrogen (Carlsbad, CA) and Pharmingen (San Diego, CA). *Spodoptera frugiperda* (Sf9) cell media was prepared by the Vanderbilt Cell Biology Core (Nashville, TN) or purchased commercially from Orbigen (San Diego, CA). Sf9 cells were purchased from Pharmingen or Orbigen. T-175 tissue culture flasks were from Corning (Corning, NY). Lysozyme type VI was from MP Biomedicals (Irvine, CA). Precision Plus All Blue protein standards and Coomassie Brilliant Blue R-250 were from Biorad (Hercules, CA). Immobilon PVDF (polyvinylidene fluoride) membranes were from Millipore (Billerica, MA). Primary antibodies used were the monoclonal anti-PDE11A antibodies 417L and 417K, which recognize the extreme C-terminus of all human PDE11A proteins (provided courtesy of Drs. Vince Florio and Kate Loughney, ICOS Co., Bothell, WA). Human His_6-tagged Met-563 to Asn-934 that contained mainly the PDE11 catalytic domain was expressed using the pET vector expression system from Novagen (San Diego, CA). Native PKG Iα that had been purified to near homogeneity was used in these studies as described previously (*27*). Centricon concentrators were from Amicon (Beverly, MA).

Construction of Recombinant Baculovirus for Sf9 Expression of Human PDE11A Isozymes. The recombinant bacu-

lovirus containing His_6-tagged PDE11A4 holoenzyme was created as described earlier (*5*). Recombinant baculoviruses expressing human non-tagged PDE11A2 and PDE11A3 were generous gifts from Drs. Kate Loughney and Vince Florio (ICOS Corp, Bothell, WA). His_6-tagged PDE11A1 was created using the human cDNA coding for full-length PDE11A4 holoenzyme used as a template with the following PCR primers to generate PDE11A1: forward primer 5′-GCTCATATGCATGTCCCCAAAGTGCAGT-3′ containing an Nde1 site (underlined) and reverse primer 5′GTAGTGGTACC**TTA**GTTCCTGTCTTCCTTGGC-3′ containing a Kpn1 site (underlined) and the stop codon (boldface type) of the human PDE11A4 sequence. This fragment was digested with Nde1 and Kpn1 and cloned into the pAcHLT-A vector (BD Pharmingen) digested by the same enzymes to yield the baculovirus expression vector, pAcHLT-A-PDE11A1. The sequence spanning PDE11A1 was verified by DNA sequencing (Vanderbilt Ingram Cancer Center DNA Sequencing Core, Vanderbilt University Medical Center, Nashville, TN). The expression vector, pAcHLT-A-PDE11A1 was then used to generate a recombinant baculovirus according to the Baculovirus Expression Vector System (Pharmingen) as described earlier.

Expression and Purification of Human PDE11A Isozymes. His_6-tagged human PDE11A4 was expressed and purified essentially as described by Ni-NTA affinity chromatograpy (*5*). We have found that the use of 1 M NaCl in the lysis buffer and Ni-NTA column buffer greatly simplifies obtaining PDE11A4 preps that are essentially free from proteolysis as evidenced by a single immunoreactive species on western blots and SDS−PAGE gels stained with silver stain. Recombinant baculoviruses for human PDE11A1, PDE11A2, and PDE11A3 were subjected to several rounds of amplification to yield high-titer baculovirus. The amount of baculovirus that yielded the highest PDE11 activity was experimentally determined for each high-titer virus versus mock-infected cells using the PDE activity assay as described (*5*).

For expression of PDE11A1 or PDE11A2, Sf9 cells were grown at 27 °C in either suspension culture at 1×10^6 cells/mL or in T-175 flasks containing 2×10^7 Sf9 cells in Grace's insect medium supplemented with 10% fetal bovine serum, 2 mM glutamine, 50 units/mL penicillin, 50 μg/mL streptomycin, and 0.125 μg/mL amphotericin B, and infected with the optimum dose of the virus. At 96 h post-infection, Sf9 cells were pelleted by centrifugation (5 min at 2000 RPM in a Beckman JA-10 rotor), the medium was removed, and the cell pellet was washed three times with ice-cold PBS (1.9 mM NaH_2PO_4, 8.1 mM Na_2HPO_4, and 150 mM NaCl at pH 7.4). Cells were snap-frozen in liquid N_2 and stored at −80 °C or lysed immediately. The cell pellet from each flask was lysed on ice for 30 min with 2 mL of lysis buffer (LB), which contained 10 mM potassium phosphate, 25 mM β-mercaptoethanol, 0.1% Triton X-100, Roche complete protease inhibitors, 0.07 μg/mL pepstatin A, 250 μM PMSF or AEBSF, 1 μg/mL leupeptin, 5 μM E-64, and 20−40 mM NaCl at a final pH of 6.8. The lysate was centrifuged at 4 °C (25 min at 10,000 RPM in a Beckman JA-20 rotor). The soluble supernatant was then diluted 1:10 in ice-cold LB lacking Triton X-100 [LB (−T)] and loaded onto a DEAE-Sephacel column (0.9 cm × 7.5 cm) that had been equilibrated in the same buffer. Several attempts were made to purify PDE11A1 using Ni-NTA resin via the His_6-tag on the vector carrying PDE11A1, but the majority of PDE11A1 that bound to the Ni-NTA could not be eluted, even upon the addition of 1 M imidazole; thus, purification using DEAE-Sephacel was adopted. After application of the sample, the column was washed first with 50 mL of LB (−T). Then the column was washed with 1.5 L of LB (−T) that contained 50 mM NaCl without protease inhibitors. PDE11A1 or PDE11A2 was eluted from the DEAE-Sephacel column with a 50−400 mM linear NaCl gradient of 72 mL in LB (−T). Fractions containing the highest PDE11 activity were pooled and dialyzed at 4 °C overnight in 2000 volumes of KPM at pH 6.8 (10 mM potassium phosphate and 25 mM β-mercaptoethanol), 150 mM NaCl, and 10% sucrose and then snap-frozen in liquid N_2. PDE activity was not affected by one freeze/thaw cycle using this freezing protocol. In some cases, fractions containing the highest PDE11A1 activity were pooled, concentrated 2−5-fold with a Centricon YM-30 concentrator, then applied to a Sephacryl S-200 gel filtration column (0.9 cm × 35 cm), and eluted with KPM containing 150 mM NaCl (pH 6.8). PDE11A1 eluted prior to the majority of the total cell protein resulting in a very effective purification step. Fractions from the Sephacryl S-200 column were used immediately or frozen as described above for PDE11A2.

PDE11A3 was very sensitive to proteolysis; cleavage was not effectively blocked despite the presence of multiple protease inhibitors in the LB. Attempts to partially purify PDE11A3 via DEAE-Sephacel chromatography using LB resulted in preparations that were markedly heterogeneous on western blots, suggesting that the low ionic strength required for the protein to bind the resin did not adequately protect PDE11A3 from proteolysis. The following method was found to be effective in obtaining partially purified preparations of PDE11A3 that were suitable for kinetic and quaternary structure studies. Sf9 cells were grown in suspension flasks as described above and infected with an optimal amount of high-titer PDE11A3 baculovirus for 96 h. Infected cells were then centrifuged (5 min at 2000 RPM in a Beckman JA-20 rotor), and the cell pellet was washed three times with PBS as described above and either snap-frozen in liquid N_2 or lysed immediately. Lysis was carried out for 5 min at 4 °C by repetitively pipetting 2.5×10^8 cells in 5 mL of LB containing 1% Triton X-100 and 1 M NaCl. This solution was then centrifuged for 30 min (28,000 RPM in a Beckman type 30 rotor), and the soluble supernatant was filtered through cheese cloth before applying to a Sephacryl S-200 column (1.7 cm × 90 cm, 125 mL bed volume) equilibrated in LB (−T) with 1 M NaCl, and fractions (1.1 mL) were collected by gravity flow. Fractions were assayed for PDE catalytic activity to determine the elution position of PDE11A3, and the identity of PDE11A3 was confirmed by western blotting using the 417L antibody. Under these conditions, PDE11A3 began eluting from the column at approximately 52 mL.

Construction, Expression and Purification of the PDE11A (Met-563 to Asn-934) Catalytic Domain. Human His_6-tagged Met-563 to Asn-934 PDE11 catalytic domain was created using the human cDNA for full-length PDE11A4 as a template to generate the Met-563 to Asn-934 region of PDE11A4 by PCR using the forward primer 5′-GTACATATGTATGATCAAGTGAAGAAGTC-3′ containing an

Nde1 site (underlined) and the reverse primer 5′-GTAGTCTC-GAG**TTA**GTTCCTGTCTTCCTTG-3′ containing an XhoI site (underlined) and the stop codon (boldface type) of the human PDE11A4 sequence. The resulting PCR fragment was digested by Nde1 and Xho1 and cloned into the pET15b vector digested with the same enzymes to yield the bacterial expression vector pET15b-PDE11 catalytic domain. The sequence corresponding to the PDE11 catalytic domain was verified by DNA sequencing. (Vanderbilt Ingram Cancer Center DNA sequencing facility, Vanderbilt University Medical Center, Nashville, TN).

The pET15b-PDE11 catalytic domain construct (120 ng) was transformed using heat-shock into 50 μL of BL21 (DE3) Codonplus RIL cells, plated on Luria−Agar plates with 50 ug/mL ampicillin, and grown overnight. A single colony was picked and added to 4 mL of Luria broth with 100 μg/mL ampicillin and 20 μg/mL chloroamphenicol (LB-AC) and grown overnight at 37 °C with shaking (250 RPM). One milliliter of this mixture was then added to 10 mL of LB-AC and grown at 37 °C overnight with shaking (250 RPM). Then, 1 mL of this mixture was added to 35 mL of LB-AC and grown at 37 °C overnight with shaking (250 RPM). Finally, 1 mL of this mixture was added to each of four Erlenmeyer flasks, each containing 1 L of LB-AC with 0.4% glucose and grown for 5.5 h at 37 °C with shaking (250 RPM). Flasks were removed from the incubator, placed on ice, and incubated at 4 °C for 40 min. Flasks were then transferred to an incubator and incubated at 11 °C for 30 min. After this, cells were induced with a final concentration of 0.1 mM IPTG and shaken at 190 RPM for 14 h at 11 °C. Cells were centrifuged at 2000 RPM for 10 min, and cells from each liter of media were resuspended in 50 mL of bacterial lysis buffer (BLB) at pH 8.0 (20 mM Tris base, 300 mM NaCl, 15 mM imidiazole, 1 mM β-mercaptoethanol, and Roche complete protease inhibitors) with 1 mg/mL lysozyme type VI and incubated on ice for 50 min. Cells were lysed by sonication using a Branson Sonifier 450 (Branson Ultrasonics Co., Danbury, CT) for 1 min four times, interspersed by cooling in an ice bath to achieve a cleared lysate that was centrifuged (20 min at 15,000 RPM in a Beckman JA-20 rotor); the soluble supernatant was saved, and the pellet was discarded. Nickel-NTA resin (1.5 mL bed volume) was then washed with 400 mL of BLB, and the washed resin was added to the soluble supernatant and gently shaken at 4 °C for 1 h. Resin was then added to a small column (0.9 × 3 cm), washed with 300 mL of BLB, and then washed with 100 mL of BLB (pH 8.0) containing 50 mM NaCl. Protein was eluted in 1 mL fractions using elution buffer at pH 8.0 (20 mM Tris-HCl, 50 mM NaCl, 150 mM imidazole, and 1 mM β-mercaptoethanol). Peak protein fractions were pooled and dialyzed for 48 h against 2000 volumes of 20 mM Tris-HCl (pH 8.0), 25 mM β-mercaptoethanol, 0.1% Triton X-100, 2 mM $MgCl_2$, 150 mM NaCl, and 10% sucrose. Aliquots were then snap-frozen in liquid N_2 and stored at −80 °C until use.

Gel Electrophoresis and Western Blots of Expressed PDE11A Isozymes. PDE11 proteins of high purity (PDE11A4, PDE11A1, and PDE11 catalytic domain) or partially purified proteins (PDE11A2, PDE11A3) were assessed by sodium dodecyl sulfate−polyacrylamide gel electrophoresis (SDS−PAGE) followed by Coomassie Brilliant Blue or silver staining and western blot analysis. Proteins were boiled for 4 min in the presence of 10% SDS, 2 mM β-mercaptoethanol, and 1% Bromophenol blue, followed by 10% SDS−PAGE and then visualized as described above. For western blot, gels were transferred to PVDF membranes and blots performed using standard protocols. Primary antibodies were used from 1000−10,000-fold dilutions. Secondary antibody was an anti-mouse conjugated to horse radish peroxidase from sheep and was used at 1000-to 3000-fold dilutions. His-tagged PDE5 (*22*) and bovine serum albumin (BSA) did not cross-react with 417L and were used as negative controls for western blots.

Measurement of PDE11 Catalytic Activity. Measurement of Michaelis−Menten constant (K_m) for cAMP or cGMP and values for IC_{50} (inhibitor concentration at 50% inhibition) of inhibitors were determined using the PDE catalytic activity assay as described previously (*5*). K_m values of human PDE11A isozymes for cGMP and cAMP were determined using cAMP and cGMP concentrations from 0.03 to 80 μM. Data for K_m studies were analyzed by nonlinear regression with a single site model in GraphPad Prism (GraphPad Software Inc., San Diego, CA). Reactions were experimentally determined to be linear with respect to time (not shown). For the determination of IC_{50} values, PDE11A isozymes were analyzed using cGMP as substrate at a concentration that was approximately 10 times below the experimentally determined K_m. This ensured that the IC_{50} value obtained approached the K_i (*28*). Data for IC_{50} studies were plotted and analyzed with GraphPad Prism using a sigmoidal dose response model. Elution positions of human PDE11A isozymes in gel filtration and sucrose gradients were determined using the PDE catalytic activity assay with 300 nM [^{3}H]cGMP as substrate. The elution position of PDE11 catalytic domain was also determined by both SDS−PAGE, followed by visualization with Coommassie Brilliant Blue and western blot analysis using the 417L antibody.

Determination of Stokes Radius of PDE11A Isozymes. PDE11A4 (1.9 μg) or partially purified PDE11A3 were combined with either catalase (4 mg) or apoferritin (2.5 mg) and cytochrome *c* (0.8 mg) in a final volume of 200 μL and loaded onto a Sephacryl S-300 gel filtration column (0.9 cm × 35 cm) equilibrated at 4 °C in 10 mM potassium phosphate, 1 mM EDTA, 25 mM β-mercapoethanol, 1 M NaCl at pH 6.8 (KPEMHS), and Roche Complete protease inhibitors. PDE11A3 and PDE11A4 were sensitive to proteolysis, which occurred during gel filtration despite the presence of several protease inhibitors and resulted either from trace amounts of proteases in the internal protein standards or from trace amounts of proteases co-purifying with these proteins. One molar NaCl in the gel filtration buffer was effective at mitigating the proteolysis of PDE11A3 and PDE11A4. The column was eluted with KPEMHS, and fractions (0.5 mL) were collected.

The Sephacryl S-300 column was standardized with protein standards of known Stokes radii: cytochrome *c* (16.6 Å), ovalbumin (29 Å), catalase (52 Å), and apoferritin (60 Å). Partially purified PDE11A2 or PDE11A1 (0.25−2 μg) was combined with various internal standards, catalase (3 mg), ovalbumin (4 mg), apoferritin (2.5 mg), cytochrome *c* (0.8 mg), or soybean trypsin inhibitor (1.75 mg) in a final volume of 200 μL and loaded onto a Sephacryl S-200 column (0.9 × 35 cm) equilibrated at 4 °C in KPEM at pH 6.8, containing 150 mM NaCl and Roche complete protease

inhibitors. The column was eluted with this buffer, and fractions (0.5 mL) were collected. The Sephacryl S-200 column was standardized with protein standards of known Stokes radii: apoferritin (60 Å), cytochrome *c* (16.6 Å), ovalbumin (29 Å), catalase (52 Å), soybean trypsin inhibitor (24.5 Å), and PKG Iα (55 Å). Protein standards were detected by spectrophotometric absorbance at 280 nm or at 411 nM for catalase and cytochrome *c*. The elution position of PKG Iα was determined by the protein kinase activity assay as described earlier (*23*). The elution position of protein standards was confirmed by SDS−PAGE followed by staining with Coomassie Brilliant Blue and scanning by a densitometry program (Scion Image, Scion Corp.). Profiles generated from spectrophotometric absorbance or densitometry scanning of SDS−PAGE gels were in excellent agreement. The PDE11 catalytic domain (65−130 μg) was combined with two internal standards, bovine serum albumin (1.75 mg) and ovalbumin (1.75 mg) in a final volume of 135 μL in KPEM with 150 mM NaCl and Roche Complete protease inhibitors and applied to a Sephadex G-100 column (0.9 × 35 cm) equilibrated in this same buffer. The column was eluted with this buffer, and fractions (0.5 mL) were collected. The Sephadex G-100 column was standardized with protein standards of known Stokes radii: soybean trypsin inhibitor (24.5 Å), bovine serum albumin monomer (35 Å), and ovalbumin (29 Å). The elution positions of the internal and external protein standards were determined as described above. Elution positions of PDE11A proteins were determined by the PDE activity assay as described above. The elution position of PDE11 catalytic domain was determined both by the PDE assay (not shown) and by western blot, with both methods agreeing well. For each gel filtration column, the thyroglobulin elution volume was taken as the void volume, and the elution volume of [^{3}H]H_2O was used to determine the inclusion volume. Elution positions of the internal protein standards were used to generate a standard curve of $(-\log K_{av})^{1/2}$ versus Stokes radius as follows:

$$K_{av} = \frac{\text{elution volume} - \text{void volume}}{\text{inclusion volume} - \text{void volume}} \quad (1)$$

The Stokes radii of PDE11A proteins were determined from the standard curve.

Determination of Sedimentation Coefficients of PDE11A Isozymes. PDE11A4 (0.003−1 μg), partially purified PDE11A2 or PDE11A3, PDE11A1 (10−100 μg), or the PDE11 catalytic domain (3−65 μg) were combined with internal standards, crystalline phosphorylase *b* (3 mg) or catalase (2 mg) and hemoglobin (0.5 mg) in a final volume of 150−200 μL in KPEM with 150 mM NaCl and Roche protease inhibitors and applied to a 13-mL linear 5−20% sucrose gradient of the same buffer, as described previously (*23*). The gradients were centrifuged at 37,000 rpm in a Beckman SW 41 Ti rotor for 19−44 h at 4 °C, and fractions (0.5 mL) were collected from the bottom of the tubes. Phosphorylase *b* has an $s_{20,w}$ value of 8.0 S and was located by absorbance at 280 nm. Catalase has an $s_{20,w}$ value of 11.5 S and was located by absorbance at 280 or 411 nm. Hemoglobin has an $s_{20,w}$ value of 3.2 S and was located by absorbance at 280 or 411 nm. The PDE catalytic activity using 300 nM [^{3}H]cGMP as substrate was used to determine the sedimentation position of PDE11 isozymes as described above.

Sedimentation coefficients of PDE11 proteins were calculated from the distance migrated into the gradients as compared with those of the standards.

Calculation of Native Molecular Weights of PDE11A Isozymes. The native molecular weights (M_r) were calculated from the experimentally determined Stokes radii and sedimentation coefficients according to the method of Siegel and Monty (*29*) using the following equation:

$$M_r = \frac{(6\pi\eta Nas)}{(1 - \nu\rho)} \quad (2)$$

where N is Avogadro's number; η is the viscosity of the medium, assumed to be 1; a is the experimentally determined Stokes radius; s is the experimentally determined sedimentation coefficient; ρ is the density of the medium, assumed to be 1; and ν is the partial specific volume, assumed to be 0.725 mL/g.

Statistical Analyses. Statisitical analysis of numerical data was performed using the unpaired Student's *t*-test function of Microsoft Excel (Redmond, WA). Error ranges presented in numerical data are ppplus or minus the standard error of the mean (S.E.M).

RESULTS

Expression and Purification of Human PDE11A Isozymes. The four human PDE11A isozymes, PDE11A1, PDE11A2, PDE11A3, and PDE11A4 (Figure 1), were expressed in Sf9 cells using baculovirus expression systems. The PDE11 catalytic domain construct (catalytic domain, Figure 1) was expressed in *Escherichia coli* using the pET vector expression system. Proteins were purified as described in Experimental Procedures. PDE11A4 and PDE11 catalytic domain were purified by Nickel-NTA column chromatography (Figure 2A). PDE11A1 was purified by DEAE-Sephacel chromatography followed by Sephacryl S-200 gel filtration (Figure 2A). PDE11A2 was partially purified using DEAE anion-exchange chromatography. PDE11A3 was partially purified by Sephacryl S-200 gel filtration in the presence of 1 M NaCl. Western blots of expressed PDE11A proteins demonstrated a single immunoreactive species for PDE11A4, PDE11A2, PDE11A1, and PDE11 catalytic domain (Figure 2B), the migration of each on SDS−PAGE agreed well with the predicted molecular weight based on amino acid composition (Table 2). PDE11A3 demonstrated a major species of approximately 75 kDa, which agreed well with the predicted molecular weight based on amino acid composition (Table 2) and two faint minor species that migrated more rapidly (Figure 2B).

Comparison of Substrate Affinities Among PDE11 Isozymes. Previous work suggested the possibility that the N-terminal domains of PDE11A isozymes affect inhibitor sensitivities and maximal velocities (*9*, *12*). Therefore, we compared in a head-to-head manner whether the N-terminal domains among the human PDE11A isozymes influence the affinity of the PDE11 catalytic site for substrates by measuring the affinities (K_m) of the respective isozymes, which have variable natural truncations, for the two substrates, cAMP and cGMP. Interestingly, PDE11 isozymes with marked truncations in their N-terminal domains (PDE11A1 and

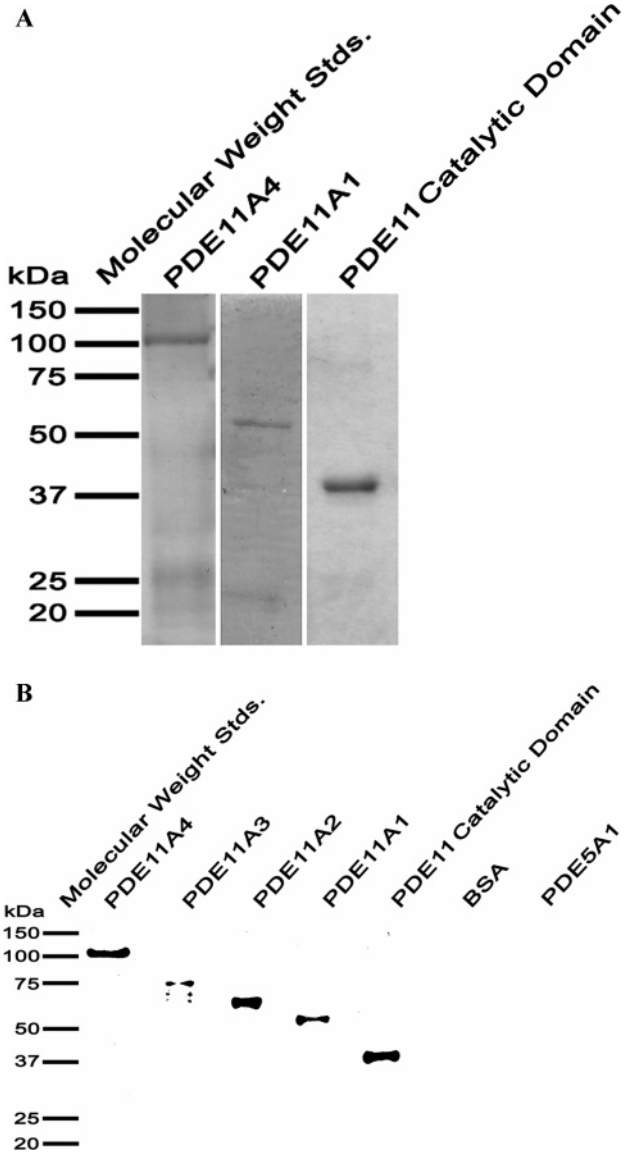

FIGURE 2: SDS−PAGE of PDE11A4, PDE11A1 and PDE11 catalytic domain and western blot of PDE11 isozymes. (A) SDS−PAGE of purified PDE11A4, PDE11A1, and the PDE11 catalytic domains. The positions of protein standards (precision plus all blue protein standards) are shown by dark bars. PDE11A4 (500 ng), PDE11A1 (2 ug), or PDE11 catalytic domain (6 μg) were mixed with loading buffer, boiled, and electrophoresed on 10% SDS−PAGE (see Experimental Procedures). PDE11A1 and PDE11 catalytic domains were detected by Coomassie Brilliant Blue stain, and PDE11A4 was detected by silver stain. (B) Western blot of expressed human PDE11A isozymes and the PDE11 catalytic domain. The positions of protein standards (precision plus all blue protein standards) are shown by dark bars. Purified PDE11A4 (0.4 μg), PDE11A1 (0.15 μg), PDE11 catalytic domains (0.13 μg) and partially purified PDE11A3 and PDE11A2 were subjected to 10% SDS−PAGE and transferred to PVDF membranes. Bovine serum albumin (BSA) (1 μg) and purified human PDE type 5A1 (PDE5A1) (1 μg) were included as negative controls. Western blots were performed according to standard protocols using the monoclonal anti-PDE11A antibody, 417L, at a dilution of 1:8333 and a dilution of 1:3000 for the secondary antibody. The blot was revealed using the Western Lightning chemiluminesence kit.

PDE11A2) displayed significantly (***$p < 0.001$) higher affinity (K_m) for cAMP (3.3−3.5-fold) and cGMP (2.5−2.9-fold) when compared directly to that of PDE11A4 (Table 1). K_m values of PDE11A3 for cGMP and cAMP were intermediate between those of PDE11A4 and the shorter isoforms PDE11A1 and PDE11A2. Although the affinities of PDE11A3 for substrates were significantly (*$p < 0.05$) lower for cGMP (2−2.3-fold) and cAMP (1.7−1.8-fold) when compared to PDE11A1 and PDE11A2, this decrease in substrate affinity was not as pronounced as that of PDE11A4. As aforementioned, we found PDE11A3 to be very sensitive to proteolysis, necessitating partial purification by gel filtration under high ionic strength conditions. To further validate the K_m determined for PDE11A3 partially purified by gel filtration, the K_m for PDE11A3 was determined using the crude supernatant immediately after lysis of PDE11A3-expressing Sf9 cells. PDE11A3 baculovirus-infected cells were lysed and centrifuged as described in Experimental Procedures. Uninfected cells were used as control to determine an appropriate dilution at which supernatant from control cells did not lead to significant hydrolysis of substrate over the blank during the assay. Using this approach, the K_m of PDE11A3 from freshly lysed cells was determined to be 0.77 ± 0.01 μM for cAMP ($n = 2$), which agreed well with the K_m (0.80 ± 0.01 μM) using cAMP as substrate from multiple experiments conducted on PDE11A3 partially purified by gel filtration (Table 1). Western blot of freshly lysed PDE11A3 cells demonstrated a single immunoreactive species (not shown), which corresponded to the major band in PDE11A3 preparations (Figure 2B) partially purified by gel filtration.

Comparison of Inhibitor Affinities Among PDE11 Isozymes. The catalytic sites of PDE11A and PDE5A share the highest sequence identity (51%) within the mammalian PDE superfamily, and moderate cross-reaction between some commercially available PDE5 inhibitors and PDE11A has been reported (*5*). To address whether differences in N-terminal domains of PDE11A isozymes affect inhibitor potency and therefore selectivity of inhibitors for PDE5 versus PDE11, we determined IC_{50} values for two structurally different inhibitors, tadalafil and vardenafil, and compared these in a head-to-head manner among the four human PDE11A isozymes (Figure 3 and Table 1). Under the conditions used, the IC_{50} of tadalafil for PDE11A4 was 73 ± 3.1 nM; this was significantly (***$p < 0.001$) less potent (3.5−4.9-fold) than the IC_{50} values determined for PDE11A2 or PDE11A1 of 21 ± 2.3 nM and 15 ± 1.5 nM, respectively. Interestingly, PDE11A3 also displayed a significant (***$p < 0.001$) and comparable increase in tadalafil potency of 3.8-fold over PDE11A4, with an IC_{50} of 19 ± 3.2 nM (Figure 3A and Table 1). Given the sensitivity of PDE11A3 to proteolysis, we determined the tadalafil IC_{50} from freshly lysed PDE11A3 baculovirus infected Sf9 cells to be 14 nM ($n = 1$), a value that agreed well with the value of 19 ± 3.2 nM from multiple experiments on PDE11A3 partially purified by gel filtration (Table 1). The potency of vardenafil, a PDE5 inhibitor that is structurally unrelated to tadalafil, for all human PDE11A isozymes was also determined in a head-to-head manner. The IC_{50} of vardenafil was 650 ± 55 nM for PDE11A4, which was significantly (***$p < 0.001$) less potent (3.9−4.3-fold) than the IC_{50} values determined for PDE11A3 (151 ± 11 nM), PDE11A2 (166 ± 12 nM), and PDE11A1 (163 ± 10 nM) (Figure 3B and Table 1). Fold differences in the potency of vardenafil between PDE11A4 and PDE11A1, and 11A2 and 11A3 agreed well with those determined for tadalafil. The vardenafil IC_{50} values determined here for PDE11A4 and PDE11A1 were in good agreement with that for

Table 1: Comparison of Substrate Affinity and Inhibitor Potency in Human PDE11 Isozymes[a]

	K_m		tadalafil	tadalafil fold selectivity	vardenafil	Vardenafil fold selectivity
	cGMP	cAMP	IC_{50}, nM	PDE5/PDE11	IC_{50}, nM	PDE5/PDE11
PDE11A4	1.0 ± 0.07	1.6 ± 0.2	73 ± 3.1	41	650 ± 55	7100
PDE11A3	0.80 ± 0.10	0.80 ± 0.01	19 ± 3.2	11	151 ± 11	1700
PDE11A2	0.34 ± 0.02	0.45 ± 0.03	21 ± 2.3	12	166 ± 12	1800
PDE11A1	0.40 ± 0.03	0.45 ± 0.05	15 ± 1.5	8	163 ± 10	1800

[a] The values are given as mean ± S.E.M. The Michealis−Menten constant (K_m) for cAMP and cGMP, inhibitor concentration at 50% inhibition (IC_{50}) value, and fold selectivity of tadalafil and vardenafil for human PDE11A isozymes were determined as described in Experimental Procedures. The results are representative of at least three experiments in which each was assayed in triplicate. Statistical significance is described in the text.

Table 2: Physical Characteristics of Human PDE11A Proteins[a]

PDE11A isozyme	predicted M_R (kDa)	SDS−PAGE M_R (kDa)	Stokes radius (Å)	sedimentation coefficient *s*	calculated M_R (kDa)	quaternary structure
PDE11A4	105	100	57.8 ± 1.25	7.9 ± 0.26	190	dimer
PDE11A3	78	75	56.1 ± 1.60	6.0 ± 0.10	140	dimer
PDE11A2	66	64	52[b]	5.2 ± 0.03	110	dimer
PDE11A1	56	55	60[c]	8.8 ± 0.03	220	tetramer
pde11cat. domain	43	45	30 ± 0.80	4.0 ± 0.12	49	monomer[d]
				6.1 ± 0.05	76	dimer[d]

[a] The values are given as mean ± S.E.M. The Stokes radius and sedimentation coefficient for each protein were used to calculate molecular mass and to determine the quaternary structure of each protein as described in Experimental Procedures. The results are representative of at least three experiments, each of which was assayed in triplicate. [b] On S-200 gel filtration, PDE11A2 essentially coelutes with the internal protein standard catalase (52 Å). [c] On S-200 gel filtration, PDE11A1 essentially coelutes with the internal protein standard apoferritin (60 Å). [d] A 1:1 ratio of monomer to dimer at 10 μM, 4:1 monomer to dimer at 2.5 μM, and all monomeric at 500 nM.

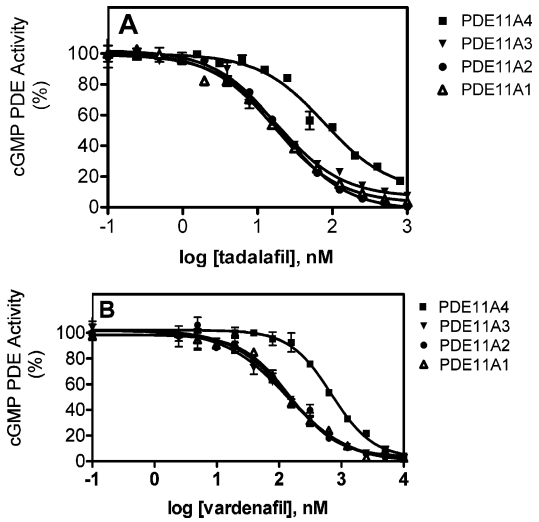

FIGURE 3: Potency of tadalafil and vardenafil for human PDE11A isozymes. The IC_{50} (inhibitor concentration at 50% inhibition) for tadalafil (panel A) and vardenafil (panel B) for PDE11A4 (■), PDE11A3 (▼), PDE11A2 (●), and PDE11A1 (Δ) was determined as described in Experimental Procedures. The errors bars are ± S.E.M., and the points without visible error bars indicate that the error is within the size of the symbol. Data plotted here are representative of at least three separate experiments, each of which was assayed in triplicate. Numerical IC_{50} values are presented in Table 1.

PDE11A4 in our previous report (*5*) and that for PDE11A1 in a report from another group (*5*, *30*).

Physical Properties of Human PDE11A Isozymes. Most mammalian PDEs that have been studied for quaternary structure are oligomeric, with the majority demonstrating a dimeric structure. GAF subdomains in the N-termini of PDE2, 5 and 6, provide important dimerization contacts in these enzymes. Three PDE11A isozymes contain one or more complete GAFs (Figure 1), but no function has been defined for these in intact PDE11A isozymes, nor has the quaternary structure of any PDE11 isozyme been delineated. To investigate the quaternary structures of human PDE11A isozymes and the potential effects of PDE11A N-terminal domains on structure, we determined the quaternary structures of the four human PDE11A isozymes as well as an N-terminal truncation mutant of PDE11A1 (PDE11 catalytic domain). Physical characteristics of human PDE11A proteins are summarized in Table 2. Stokes radii of human PDE11A proteins were determined by gel filtration chromatography as described in Experimental Procedures. PDE11A4 and PDE11A3 were each chromatographed on a Sephacryl S-300 column and both eluted between the internal standards apoferritin (60 Å) and cytochrome *c* (16.6 Å) with Stokes radii of 57.8 Å for PDE11A4 (Figure 4A, Table 2) and 56.1 Å for PDE11A3 (Figure 4B, Table 2). On Sephacryl S-200 gel filtration chromatography, PDE11A2 essentially coeluted with the internal standard catalase with a Stokes radius of 52 Å (Figure 4C, Table 2). Interestingly, on Sephacryl S-200 gel filtration, PDE11A1 essentially coeluted with the internal standard apoferritin with a Stokes radius of 60 Å (Fig, 4D, Table 2); this value was higher than that of PDE11A2, PDE11A3, or PDE11A4 despite PDE11A1 having the lowest predicted subunit molecular weight of the four isozymes. The PDE11 catalytic domain was chromatographed on both a Sephadex G-100 and Sephacryl S-100 gel filtration column along with internal standards bovine serum albumin monomer (35 Å), ovalbumin (29 Å), soybean trypsin inhibitor (24.5 Å), and cytochrome *c* (16.6 Å). The Stokes radius of the PDE11 catalytic domain determined in this manner was 30 Å (Table 2), and the elution position was detected both by western blot analysis (Figure 5A) and the PDE activity assay (not shown), with both methods agreeing well.

Sucrose density gradient centrifugation was performed as described in Experimental Procedures, to determine the

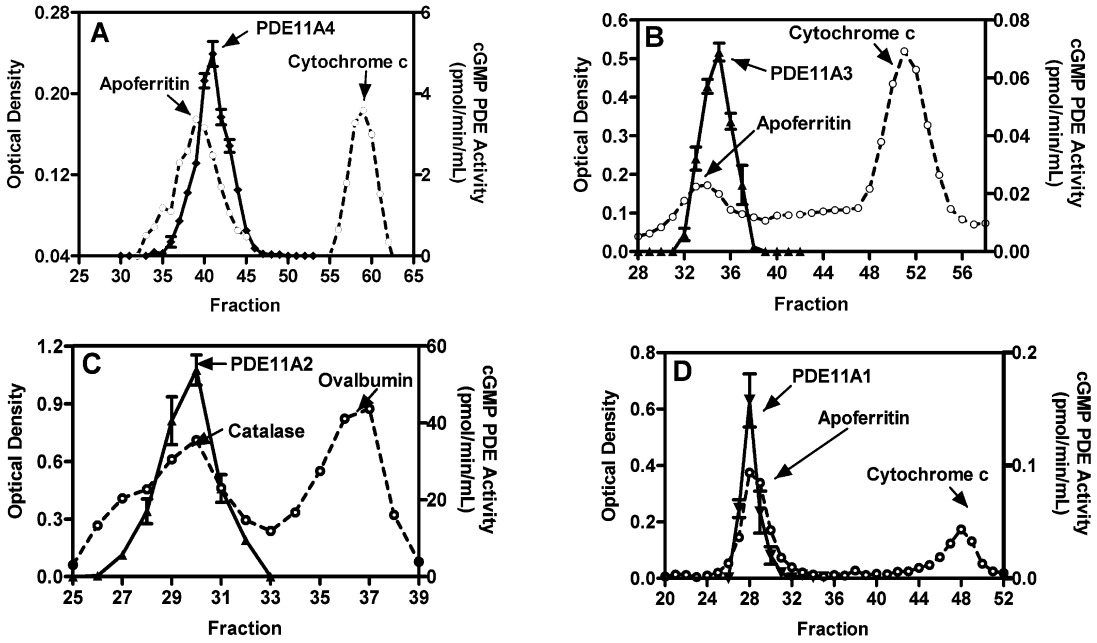

FIGURE 4: Gel filtration of human PDE11A isozymes. Human PDE11 proteins were combined with the indicated protein standards and subjected to gel filtration chromatography as described in Experimental Procedures. Sephacryl S-300 column chromatography was used for PDE11A4 (panel A) or PDE11A3 (panel B). Sephacryl S-200 chromatography was used for PDE11A2 (panel C) or PDE11A1 (panel D). Fractions (0.5 mL) were collected and assayed for PDE activity as described in Experimental Procedures. Protein standards were detected by spectrophotometric absorbance at 280 nm or 411 nm, and peaks were confirmed by 10% SDS−PAGE followed by Coomassie Brilliant Blue staining. The results are representative of three or more separate experiments, each of which was assayed in triplicate.

sedimentation coefficients (*s*-values) of human PDE11A isozymes (Table 2). PDE11A4 and PDE11A3 sedimented between catalase (11.5 S) and hemoglobin (3.2 S) with calculated sedimentation coefficients of 7.9 and 6.0 S, respectively (Figure 6A and B, Table 2). PDE11A2 sedimented between phosphorylase *b* (8.0 S) and hemoglobin (3.2 S) with a calculated sedimentation coeffecient of 5.2 S (Figure 6C, Table 2). Suprisingly, PDE11A1 sedimented faster than phosphorylase *b* (8.0 S), and when centrifuged in the presence of catalase (11.5 S) and hemoglobin (3.2 S), the *s*-value of PDE11A1 was determined to be 8.8 S (Figure 6D, Table 2). The PDE11 catalytic domain demonstrated heterogeneity in sucrose gradients with a 4.0 S component and a heavier component of 6.1 S. (Figure 5B, Table 2). When the concentration of the PDE11 catalytic domain applied to the gradients was decreased from 10 μM (Figure 5B) to 2.5 μM (Figure 5C), the PDE activity shifted mainly to the lighter component, suggesting that the two components were in equilibrium and that the lower concentration favored the formation of the lighter component. Both peaks were inhibited by tadalafil and could be visualized on western blots using the 417L antibody (not shown). The profile generated from the PDE activity assay in Figures 5B and 5C agreed well with that in which the elution position of PDE11 catalytic domain was determined by western blot or SDS−PAGE followed by staining with Coomassie Brilliant Blue or silver stain (not shown). To estimate the ratio of each component in the gradients containing 10 μM and 2.5 μM PDE11 catalytic domain, we determined the area under the curve (AUC) as described earlier (*31*). AUC determination based on the PDE activity profile from multiple sucrose gradients demonstrated that when 10 μM PDE11 catalytic domain (Figure 5B) was applied to the gradients the two components were present at an approximate ratio of 1:1. When the concentration of the PDE11 catalytic domain applied to the gradients was reduced to 2.5 μM, the ratio shifted to 4-fold, with the lighter component predominating (Figure 5C). When 0.5 μM PDE11 catalytic domain was applied, the protein sedimented almost exclusively as the apparent monomeric component when detected by western blot using the 417L antibody (not shown), which suggested that the dimeric component had dissociated into the monomer.

The quaternary structure of human PDE11A proteins was calculated according to the method of Siegel and Monty (see Experimental Procedures), which utilizes both the experimentally determined Stokes radius and sedimentation coefficient to calculate native molecular weight (*29*). The quaternary structure can then be assigned on the basis of the comparison with the molecular weight of the subunit predicted from amino acid composition. The calculated native molecular weights of PDE11A4 (190 kDa), PDE11A3 (140 kDa), and PDE11A2 (110 kDa) were approximately double their predicted molecular weights based on amino acid sequence (Table 2) and migration on SDS−PAGE (Figure 2B); these values were therefore consistent with a dimeric quaternary structure. Interestingly, the native molecular weight of PDE11A1 was 220 kDa, which was consistent with a tetrameric quaternary structure. The PDE11 catalytic domain construct was assigned a monomer/dimer quaternary structure, with a monomeric 49-kDa component having a molecular weight similar to that determined by SDS−PAGE, predicted amino acid molecular weight, and a second dimeric component of 76 kDa (Table 2).

In order to estimate the concentrations of PDE11 isozymes in quaternary structure studies and arrive at a minimum estimate of the affinity of oligomerization, we determined the specific activities of purified PDE11A4, PDE11A1, and PDE11 catalytic domain. On the basis of protein determination by Bradford assay, the specific activity of PDE11A4

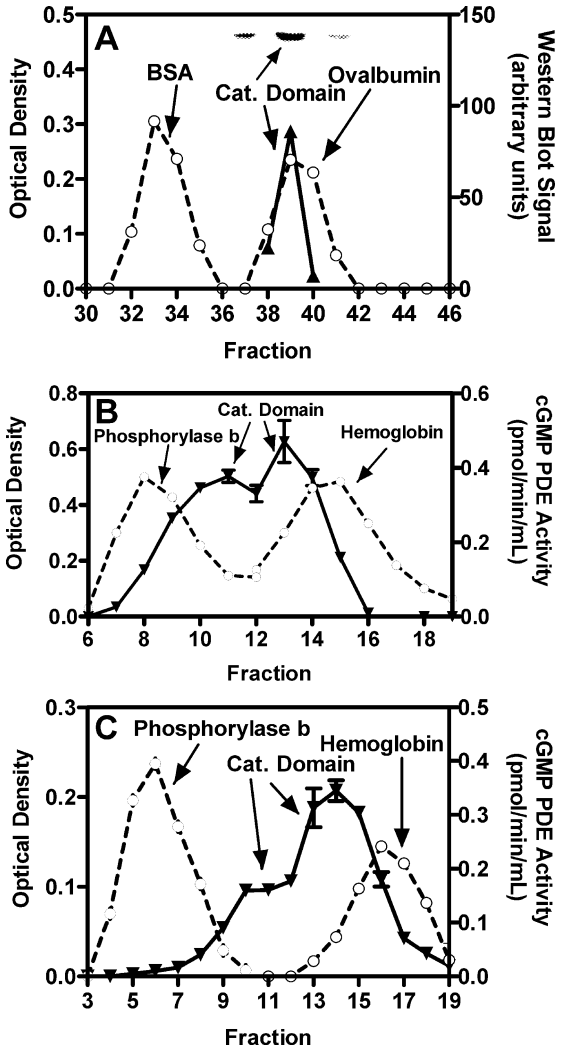

FIGURE 5: Sucrose gradient centrifugation and gel filtration chromatography of the PDE11 catalytic domain. (A) Sephadex G-100 gel filtration of 10 μM PDE11 catalytic domain in the presence of two internal standards, bovine serum albumin monomer (35 Å), and ovalbumin (29 Å). The elution position of PDE11 catalytic domain was detected by western blotting with the 417L antibody (see western blot insert at top of figure) and confirmed by SDS−PAGE, followed by staining with Coomassie Brilliant Blue stain, which agreed well with the elution position determined by the PDE activity assay (not shown). Sucrose gradients were performed as described in Experimental Procedures. Sucrose gradient centrifugation of the PDE11 catalytic domain (panels B and C) was conducted in the presence of two internal standards, phosphorylase *b* (8 S) and hemoglobin (3.2 S). The concentration of PDE11 catalytic domain in the applied sample was 10 μM for panel B and 2.5 μM for panel C. The results are representative of three separate experiments, each of which was assayed in triplicate.

was estimated to be 0.29 μmol/min/mg for cGMP (k_{cat} of 0.51 s^{-1} for cGMP) and 2−10-fold higher for cAMP. When the specific activity of PDE11A1 was estimated in the same manner, the value obtained was 0.0058 μmol/min/mg for cGMP (k_{cat} of 0.0054 s^{-1} for cGMP) and 1.6-fold higher for cAMP. The specific activities reported here as well as the substantial difference in specific activity between PDE11A4 and PDE11A1 agree with previous reports using the partially purified enzymes (*9*, *11*, *12*). The PDE11 catalytic domain construct showed no preference for either cAMP or cGMP, with estimated specific activities of 0.00026 μmol/min/mg for both cAMP and cGMP (k_{cat} of 0.00019 s^{-1}). Estimates of enzyme concentration based on the specific activity of PDE11A4 revealed that this isozyme remained dimeric at 3.3 pM on sucrose gradients (Figure 6A), indicating that the K_D for dimerization was less than 3 pM. By gel filtration chromatography, PDE11A1 remained tetrameric at 3.3 nM (Figure 4D), indicating that the K_D for oligomerization was less than 3.3 nM. Similarly, sucrose gradients of PDE11A1 revealed that the enzyme remained oligomeric at low nanmolar (18.4 nM) concentrations (Figure 6D). In contrast to PDE11A4 and PDE11A1, the PDE11 catalytic domain segregated in sucrose gradients into monomeric and dimeric species at much higher concentrations of 1.0 and 0.7 μM, respectively (Figure 5B). Assuming that these two species represent the monomeric and dimeric forms in equilibrium, it can be concluded that the K_D for dimerization in the PDE11 catalytic domain is in this range of 0.7−1.0 μM.

DISCUSSION

The work presented herein is the first to demonstrate differences in the affinities of the four naturally occurring PDE11 isozymes for both substrates and inhibitors. On the basis of comparisons of the affinity for either cAMP or cGMP of PDE11A4 with that of the naturally occurring truncated isozymes, PDE11A1 and PDE11A2, it has been found that residues 1−358 of PDE11A4 have an inhibitory effect on substrate affinity. The results of studies using two structurally unrelated inhibitors, tadalafil and vardenafil, demonstrate that the presence of a similar inhibitory region of PDE11A4 (residues 1−304) also decreases the potency of these inhibitors with respect to PDE11A3, PDE11A2, and PDE11A1, in which this region is absent.

The substantial difference in specific enzyme activity between PDE11A4 and PDE11A1 that we observe has been described in a previous report (*12*); taken together, these data suggest that the N-terminal 444 residues of PDE11A4 may contain a region that is required for full catalytic activity. It is unlikely that this difference results from misfolding or other perturbations of the PDE11A1 catalytic site since the affinities for substrate and several inhibitors are actually improved when compared directly to those of PDE11A4. With respect to other PDEs, the deletion of large parts of the N-terminal domains of PDE1, PDE2, and PDE5 does not significantly change the specific enzyme activity relative to wild type, while reports suggest that N-terminal truncations in PDE3 and PDE4 actually increase specific enzyme activity (*32*−*38*). It is unknown whether the 28−45-fold difference in k_{cat} using cGMP or cAMP as substrate that is observed between PDE11A1 and the PDE11 catalytic domain is due to further truncation of the N-terminal domain or to different expression and purification procedures. When the IC_{50} of tadalafil for the PDE11 catalytic domain is determined using cGMP as substrate, the value obtained from three separate experiments is 27 ± 3.6 nM, which agrees well with values obtained from the PDE11A isozymes other than PDE11A4 (Table 1) and suggests that the catalytic site is intact as determined by tadalafil inhibition. However, caution is suggested when comparing the specific activity and inhibitor potency between the catalytic domain and PDE11A1−PDE11A4 since expression and purification procedures were different.

These studies are the first to investigate the quaternary structure of any PDE11 isozyme and provide new insights

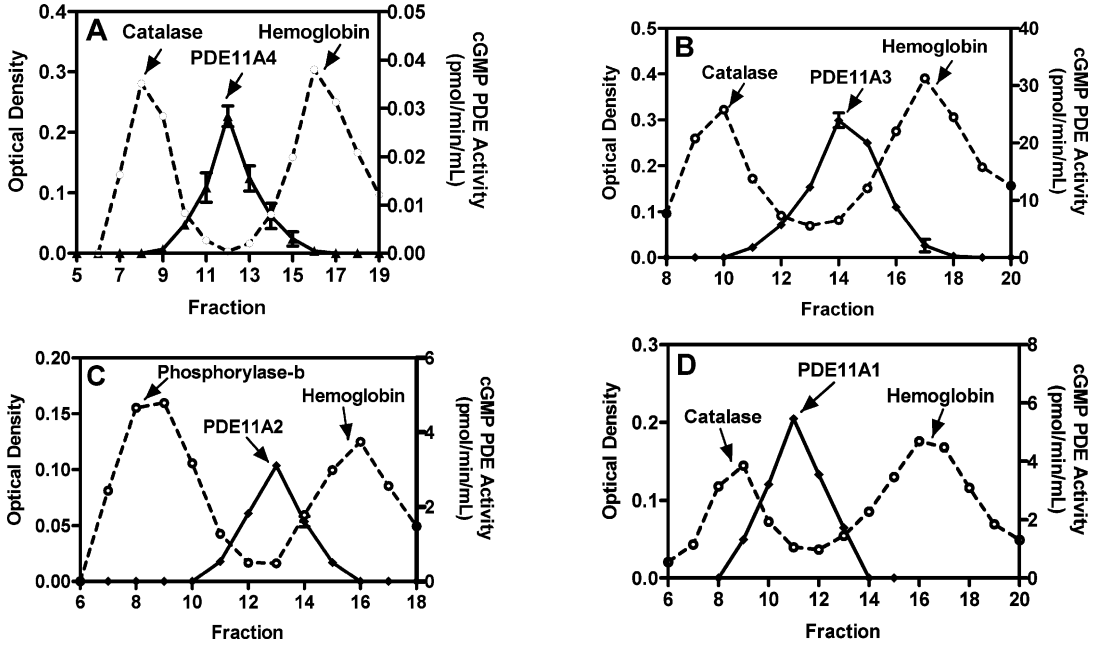

FIGURE 6: Sucrose density centrifugation of human PDE11A isozymes. PDE11A4 (panel A), PDE11A3 (panel B), PDE11A2 (panel C), and PDE11A1 (panel D) were subjected to sucrose density centrifugation (5−20%) as described in Experimental Procedures. Protein standards, catalase (2 mg) or crystalline phosphorylase *b* (3 mg), and hemoglobin (0.5 mg) were run in each gradient as internal controls. Following centrifugation, fractions (0.5 mL) were collected, and the elution positions of PDE11A proteins were determined by the PDE activity assay as described in Experimental Procedures. Protein standards were determined by spectrophotometric absorbance at 280 nm or 411 nm, and peaks were further verified by 10% SDS−PAGE followed by Coomassie Brilliant Blue staining. The results are representative of at least three experiments, each of which was assayed in triplicate.

about oligomerization contacts in this PDE family. First, PDE11A isozymes with truncations in GAF-A (PDE11A3 and PDE11A2) or the complete absence of GAF-A (PDE11A1) are oligomers, indicating that GAF-A is not required for the formation of oligomers in human PDE11A isozymes. While not required for oligomerization, a contribution of GAF-A to the affinity of oligomerization, as occurs in PDE5 (*17*), cannot be excluded. Second, our data suggest that oligomerization of PDE11A isozymes is due to high-affinity (K_D < 3 pM) interactions since the sedimentation coefficient of PDE11A4 is unchanged at concentrations in the low picomolar (3 pM) range, which agrees well with our previous studies on the affinity of the dimerization of PDE5 constructs (*17*). The shortest isoform, PDE11A1, is oligomeric at low (3.3 nM) concentrations during gel filtration, indicating that the C-terminal 123 amino acids of GAF-B are sufficient to mediate high-affinity (K_D < 3.3 nM) oligomerization. However, a contribution of the intervening sequence, between the GAFs or within the GAF-B region, on the affinity of oligomerization cannot be excluded. Results of studies on the PDE11 catalytic domain are consistent with the possibility of low-affinity oligomerization contacts within this construct (residues 563−934 of human PDE11A4) but suggest that the main oligomerization contacts reside within the N-terminal domains of PDE11 isozymes. The isolated catalytic domains of several PDEs (PDE1, PDE3, PDE4, and PDE9) are oligomeric in their respective crystal structures (*36*, *39*−*41*), while the catalytic domain of PDE5 exists as a monomer in both solution and crystal structures (*36*, *37*).

The oligomerization state of several PDEs as well as that of many other enzyme families has been shown to affect regulatory mechanisms and sensitivity to ligands, providing a rationale for the investigation of the relationship of oligomeric structure and catalytic function in PDE11 isozymes. The PDE4 family consists of long and short forms that differ in the length of an N-terminal domain; the short forms are monomers, while the long forms are oligomers. In the PDE4 family, the oligomeric state has been shown to have important functional consequences, whereas the short monomeric forms lack certain forms of regulation and show decreased potency for certain inhibitors but retain similar affinities for the substrate, cAMP (*21*). In solution, PDE5 exists as a homodimer composed of two subunits of approximately 100 kDa. Dimerization in PDE5 occurs exclusively within the N-terminal domain, and a construct containing only the PDE5 catalytic domain exists as a monomer both in solution studies and in X-ray crystallographic studies (*17*, *22*, *36*, *37*). Interestingly, the monomeric PDE5 catalytic domain domain shows substantially decreased potency for vardenafil while retaining the affinity of the holoenzyme for the substrate, cGMP, or other classes of inhibitors (*22*). In PKG Iβ, dimerization is an important regulatory feature and increases affinity for allosteric cGMP binding and activation of the enzyme (*23*). It is of interest to note that the catalytic effects (described herein) resulting from the naturally truncated isozymes of PDE11 are apparently not the result of clear differences in their oligomeric state since PDE11A2 (dimeric) and PDE11A1 (tetrameric) both show increased affinity for substrate and inhibitors when compared to that shown by PDE11A4 (dimeric). Furthermore, the PDE11 catalytic domain at higher concentrations exists as a monomer/dimer yet still retains the increased affinity for tadalafil that is seen with PDE11A3, PDE11A2, and PDE11A1. At least two possibilities can account for these differences: first, an N-terminal region of PDE11A4 that is absent in shorter isozymes may cause a structural change that is transduced to the catalytic domain, and second, this N-terminal region of PDE11A4 may have a direct

physical interaction with the catalytic domain. The lowering of ligand affinity of the catalytic site by elements within the N-terminal region of PDE11A4 is consistent with the presence of an inhibitory subdomain in this region. This inhibition could be relieved by modulatory effects such as allosterism (*19*) or covalent modifications, although such mechanisms have yet to be demonstrated in intact PDE11 isozymes.

As aforementioned, the catalytic site of PDE11 is most closely related to the catalytic site of PDE5. Since the biochemical characteristics and physiological roles of PDE11 isozymes are not well understood (*5*), cross-reaction of PDE11 isozymes with commercially available PDE5 inhibitors (*5*, *42*−*44*), such as tadalafil, has been a concern. A tadalafil PDE5/PDE11 selectivity ratio of 5-fold using PDE11A1 has been reported (*30*), whereas we have reported that this is 41-fold when comparing PDE5 and PDE11A4 (*5*). This higher selectivity ratio makes significant cross-reaction of tadalafil with PDE11A4 less likely. Recently, two independent reports have demonstrated that PDE11A4 is the most readily detected PDE11 isozyme in human tissues (*24*, *25*). The present study provides the first direct pharmacological comparison of the potency of tadalafil (and vardenafil) for all human PDE11 isozymes and demonstrates that the fold-selectivity of these widely distributed PDE5 inhibitors for PDE5 versus PDE11 depends on the particular isozyme of PDE11 that is considered (Table 1).

In conclusion, the results presented herein demonstrate the importance of the N-terminal domains of human PDE11A isozymes not only for quaternary structure but also for influencing the affinity for substrate as well as potency and selectivity of inhibitors. This emphasizes the importance of evaluating affinity for substrates and inhibitors in the context of varied N-terminal domains within the PDE11 family.

ACKNOWLEDGMENT

We kindly acknowledge Drs. Vince Florio and Kate Loughney of ICOS Co., and Drs. Kenji Omori and Jun Kotera of Tanabe Seiyaku Co. Ltd. for providing several PDE11A reagents. We also thank Dr. Raja Konjeti for synthesizing tadalafil.

REFERENCES

1. Francis, S. H., Turko, I. V., and Corbin, J. D. (2001) Cyclic nucleotide phosphodiesterases: relating structure and function, *Prog. Nucleic Acid Res. Mol. Biol. 65*, 1−52.
2. Rybalkin, S. D., Yan, C., Bornfeldt, K. E., and Beavo, J. A. (2003) Cyclic GMP phosphodiesterases and regulation of smooth muscle function, *Circ. Res. 93*, 280−291.
3. Soderling, S. H., and Beavo, J. A. (2000) Regulation of cAMP and cGMP signaling: new phosphodiesterases and new functions, *Curr. Opin. Cell Biol. 12*, 174−179.
4. Beavo, J. A., Conti, M., and Heaslip, R. J. (1994) Multiple cyclic nucleotide phosphodiesterases, *Mol. Pharmacol. 46*, 399−405.
5. Weeks, J. L., Zoraghi, R., Beasley, A., Sekhar, K. R., Francis, S., and Corbin, J. (2005) High biochemical selectivity of tadalafil, sildenafil and vardenafil for human phosphodiesterase 5A1 (PDE5) over PDE11A4 suggests the absence of PDE11A4 crossreaction in patients, *Int.J. Impotence Res. 14*, 5−9.
6. Conti, M., and Beavo, J. (2007) Biochemistry and physiology of cyclic nucleotide phosphodiesterases: essential components in cyclic nucleotide signaling, *Annu. Rev. Biochem.*, in press.
7. Weeks, J. L., Blount, M. A., Rouse, A. B., Zoraghi, R., Thomas, M. K., Sekhar, K. R., Corbin, J. D., and Francis, S. H. (2005) *Radiolabeled Ligand Binding to the Catalytic or Allosteric Sites of PDE5 and PDE11*, Humana Press, Totowa, NJ.
8. Yuasa, K., Kanoh, Y., Okumura, K., and Omori, K. (2001) Genomic organization of the human phosphodiesterase PDE11A gene. Evolutionary relatedness with other PDEs containing GAF domains, *Eur. J. Biochem. 268*, 168−178.
9. Yuasa, K., Kotera, J., Fujishige, K., Michibata, H., Sasaki, T., and Omori, K. (2000) Isolation and characterization of two novel phosphodiesterase PDE11A variants showing unique structure and tissue-specific expression, *J. Biol. Chem. 275*, 31469−31479.
10. Hetman, J. M., Robas, N., Baxendale, R., Fidock, M., Phillips, S. C., Soderling, S. H., and Beavo, J. A. (2000) Cloning and characterization of two splice variants of human phosphodiesterase 11A, *Proc. Natl. Acad. Sci. U.S.A. 97*, 12891−12895.
11. Fawcett, L., Baxendale, R., Stacey, P., McGrouther, C., Harrow, I., Soderling, S., Hetman, J., Beavo, J. A., and Phillips, S. C. (2000) Molecular cloning and characterization of a distinct human phosphodiesterase gene family: PDE11A, *Proc. Natl. Acad. Sci. U.S.A. 97*, 3702−3707.
12. Yuasa, K., Ohgaru, T., Asahina, M., and Omori, K. (2001) Identification of rat cyclic nucleotide phosphodiesterase 11A (PDE11A): comparison of rat and human PDE11A splicing variants, *Eur. J. Biochem. 268*, 4440−4448.
13. Zoraghi, R., Corbin, J., and Francis, S. (2004) Properties and functions of GAF domains in cyclic nucleotide phosphodiesterases and other proteins, *Mol. Pharmacol. 65*, 267−278.
14. Cote, R. (2004) Characteristics of photoreceptor PDE (PDE6): similarities and diffrrences to PDE5, *Int. J. Impotence Res. 16*, S28−S33.
15. Martinez, S. E., Hol, W. G., and Beavo, J. (2002) GAF domains: two-billion-year-old molecular switches that bind cyclic nucleotides, *Mol. Interventions 2*, 317−323.
16. Martinez, S. E., Wu, A. Y., Glavas, N. A., Tang, X. B., Turley, S., Hol, W. G., and Beavo, J. A. (2002) The two GAF domains in phosphodiesterase 2A have distinct roles in dimerization and in cGMP binding, *Proc. Natl. Acad. Sci. U.S.A. 99*, 13260−13265.
17. Zoraghi, R., Bessay, E., Corbin, J., and Francis, S. (2005) Structural and functional features in human PDE5A1 regulatory domain that provide for allosteric cGMP binding, dimerization, and regulation, *J. Biol. Chem. 280*, 12051−12063.
18. Muradov, K. G., Boyd, K. K., Martinez, S. E., Beavo, J. A., and Artemyez, N. O. (2003) The GAFa domains of rod cGMP-phosphodiesterase 6 determine the selectivity of the enzyme dimerization, *J. Biol. Chem. 278*, 10594−10601.
19. Gross-Langenhoff, M., Hofbauer, K., Weber, J., Schultz, A., and Schultz, J. (2006) cAMP is a ligand for the tandem GAF domain of human phosphodiesterase 10 and cGMP for the tandem GAF domain of phosphodiesterase 11, *J. Biol. Chem. 281*, 2841−2846.
20. Richter, W. (2005) *Methods in Molecular Biology: Phosphodiesterase Methods and Protocols* (Lugnier, C., Ed.) pp 167−180, Humana Press, Totowa, NJ.
21. Richter, W., and Conti, M. (2004) The oligomerization state determines regulatory properties and inhibitor sensitivity of type 4 cAMP-specific phosphodiesterases, *J. Biol. Chem. 279*, 30338−30348.
22. Blount, M., Zoraghi, R., Ke, H., Bessay, E., Corbin, J., and Francis, S. (2006) A 46-amino acid segment in phosphodiesterase-5 GAF-B domain provides for high vardenafil potency over sildenafil and tadalafil and is involved in phosphodiesterase-5 dimerizatio, *Mol. Pharmacol. 70*, 1822−1831.
23. Richie-Jannetta, R., Francis, S., and Corbin, J. (2003) Dimerization of cGMP-dependent protein kinase Ibeta is mediated by an extensive amino-terminal leucine zipper motif, and dimerization modulates enzyme function, *J. Biol. Chem. 278*, 50070−50079.
24. Loughney, K., Taylor, J., and Florio, V. (2005) 3′, 5′-cyclic nucleotide phosphodiesterase 11A: localization in human tissues, *Int. J. Impotence Res. 17*, 320−325.
25. D'Andrea, M., Qiu, Y., Haynes-Johnson, D., Bhattacahrjee, S., and Lundeen, S. (2005) Expression of PDE11A in normal and malignant human tissues, *J. Histochem. Cytochem. 53*, 895−903.
26. Daugan, A.-M. (2000) Use of cGMP-Phosphodiesterase in Methods and Compositions to Treat Impotence, ICOS Corp., U.S. Patent 6,140,329.
27. Francis, S. H., Wolfe, L., and Corbin, J. D. (1991) Purification of type I alpha and type I beta isozymes and proteolyzed type I beta monomeric enzyme of cGMP-dependent protein kinase from bovine aorta, *Methods Enzymol. 200*, 332−341.
28. Bush, K. (1983) Screening and characterization of enzyme inhibitors as drug candidates, *Drug Metab. Rev. 14*, 689−708.
29. Siegel, L. M., and Monty, K. J. (1966) Determination of molecular weights and frictional ratios of proteins in impure systems by use

of gel filtration and density gradient centrifugation. Application to crude preparations of sulfite and hydroxylamine reductases, *Biochim. Biophys. Acta 112*, 346−362.
30. Gbekor, E., Bethell, S., Fawcett, L., Mount, N., and Phillips, S. (2002) Selectivity of sildenafil and other phosphodiesterase type 5 (PDE5) inhibitors against all human phosphodiesterase families, *Eur. Urol. Suppl. 1*, 63.
31. Corbin, J. D., Soderling, T. R., and Park, C. R. (1973) Regulation of adenosine 3′,5′-monophosphate-dependent protein kinase. I. Preliminary characterization of the adipose tissue enzyme in crude extracts, *J. Biol. Chem. 248*, 1813−1821.
32. Cheung, P. P., Xu, H., McLaughlin, M. M., Ghazaleh, F. A., Livi, G. P., and Colman, R. W. (1996) Human platelet cGI-PDE: expression in yeast and localization of the catalytic domain by deletion mutagenesis, *Blood 88*, 1321−1329.
33. Iffland, A., Kohls, D., Low, S., Luan, J., Zhang, Y., Kothe, M., Cao, Q., Kamath, A. V., Ding, Y.-H., and Ellenberger, T. (2005) Structural Determinants for inhibitor specificity and selectivity in PDE2A using the wheat germ in vitro translation system, *Biochemistry 44*, 8312−8325.
34. Jin, S. L., Swinnen, J. V., and Conti, M. (1992) Characterization of the structure of a low Km, rolipram-sensitive cAMP phosphodiesterase. mapping of the catalytic domain, *J. Biol. Chem. 267*, 18929−18939.
35. Kovala, T., Sanwal, B. D., Ball, E. H., Lorimer, I. A., and Brickenden, A. M. (1997) Recombinant expression of a type IV, cAMP-specific phosphodiesterase: characterization and structure-function studies of deletion mutants, *Biochemistry 36*, 2968−2976.
36. Huai, Q., Liu, Y., Francis, S., Corbin, J., and Ke, H. (2003) Crystal structures of phosphodiesterases 4 and 5 in complex with inhibitor 3-isobutyl-1-methyxanthine suggest a conformation determinant of inhibitor selectivity, *J. Biol. Chem. 279*, 13095−13101.
37. Fink, T. L., Francis, S. H., Beasley, A., Grimes, K. A., and Corbin, J. D. (1999) Expression of an active, monomeric catalytic domain of the cGMP-binding cGMP-specific posphodiesterase (PDE5), *J. Biol. Chem. 274*, 34613−34620.
38. Sonnenburg, W. K., Seger, D., Kwak, K. S., Huang, J., Charbonneau, H., and Beavo, J. A. (1995) Identification of inhibitory and calmodulin-binding domains of the PDE1A1 and PDE1A2 calmodulin-stimulated cyclic nucleotide phosphodiesterases, *J. Biol. Chem. 270*, 30989−31000.
39. Huai, Q., Wang, H., Zhang, W., Colman, R. W., Robinson, H., and Ke, H. (2004) Crystal structure of phosphodiesterase 9 shows orientation variation of inhibitor 3-isobutyl-1-methyxanthine binding, *Proc. Natl. Acad. Sci. U.S.A. 101*, 9624−9629.
40. Scapin, G., Patel, S., Chung, C., Varnerin, J., Edmondson, S., Mastracchio, A., Parmee, E., Singh, S., Becker, J., Van der Ploeg, L., and Tota, M. (2004) Crystal structure of human phosphodiesterase 3B: atomic basis for substrate and inhibitor specificity, *Biochemistry 43*, 6091−6100.
41. Zhang, K., Card, G. L., Suzuki, Y., Artis, D. R., Fong, D., Gillette, S., Hsieh, D., Neiman, J., West, B. L., Zhang, C., Milburn, M. V., Kim, S.-H., Schlessinger, J., and Bollag, G. (2004) A glutamine switch mechanism for nucleotide selectivity by phosphodiesterases, *Mol. Cell 15*, 279−286.
42. Hellstrom, W., Oversreet, J. W., Yu, A., Saikali, K., Shen, W., Beasley, C. M., and Watkins, V. S. (2003) Tadalafil has no detrimental effect on human spermatogenesis or reproductive hormones, *J. Urol. 170*, 887−891.
43. Pomara, G., and Morelli, G. (2004) Re: tadalafil has no detrimental effect on human spermatogenesis or reproductive hormones, *J. Urol. 171*, 2390−2391.
44. Pomara, G., and Morelli, G. (2005) Inhibition of phosphodiesterase 11 (PDE11) impacts on sperm quality, *Int. J. Impotence Res. 17*, 385−386.

BI7009629